# Asymmetric Thermal Stresses of Hollow FGM Cylinders with Piezoelectric Internal and External Layers

M. Jabbari [*], M.B. Aghdam

*Postgraduate School, Islamic Azad University, South Tehran Branch, Iran*

**ABSTRACT**

In this paper ,the general solution of steady-state one dimensional asymmetric thermal stresses and electrical and mechanical displacements of a hollow cylinder made of functionally graded material and piezoelectric layers is developed .The material properties ,except the Poisson's ration, are assumed to depend on the variable radius and they are expressed as power functions of radius. The temperature distribution is assumed to be a function of radius with general thermal and mechanical boundary conditions on the inside and outside surfaces. By using the separation of variables method and complex Fourier series, the Navier equations in term of displacements are derived and solved.

© 2015 IAU, Arak Branch.All rights reserved.

**Keywords :** Hollow cylinder ; Asymmetric ; FGM ; Piezoelectric.

## 1 INTRODUCTION

FUNCTIONALLY graded materials(FGMs) have attracted widespread attention in recent years. They are new, advanced, heat resisting materials used in modern technologies as advanced structures such as chemical plants, electronics, biomaterials, and so on.

A FGM is usually a combination of two material phases in which the elastic and thermal properties change from one surface to the other, gradually and continuously. The body is constructed by smoothly changing materials. Since ceramics has good heat resistance and metal has high strength, the ceramic-metal FGM may work at super high-temperatures or under high-temperature gradient field. Several investigators represent analytical solutions about these kinds of material [1-3]. Piezoelectric materials are widely used due to their direct and inverse effects. The use of piezoelectric layers as distributed sensors and actuators in structures to control noise and deformations and suppress vibrations is quite common. In effect, the governing equation for the temperature and stress distributions are coordinate dependent as the material properties are functions of position. The classical method of analysis is to combine the equilibrium equations with the stress-strain and strain-displacement relations to arrive at the governing equations in terms of the displacement components, called the navier equations. Several research works have been contributed to model and investigate the basic structural responses of piezoelectric materials i.e. in the pioneering researches of Tiersten [4]. Kapuria et al. [5] presented an exact solution for a finite simply supported, transversely isotropic cylindrical shell subjected to axisymmetric thermal, pressure and electrostatic loading. The analytical solution for the stresses of FGMs in the one-dimensional case for spheres and cylinders are given by Lutz and Zimmerman [6,7]. Jabbari et al. [8] studied a general solution for mechanical and thermal stresses in a functionally

---

[*] Corresponding author. Tel.: +98 9122447595.
*E-mail address: mohsen.jabbari@gmail.com* (M. Jabbari).

graded hollow cylinder due to nonaxisymmetric steady-state load. They applied separation of variables and the complex Fourier series to solve the heat conduction and Navier equations. Jabbari et al. [9] also studied the mechanical and thermal stresses in functionally graded hollow cylinder due to radially symmetric loads. They assumed the temperature distribution to be a function of radial direction. They applied a method to solve the heat conduction and Navier equations. Also , Jabbari et al. [10] studied the axisymmetric mechanical and thermal stresses in thick short length functionally graded material cylinder. They applied the method of separation of variables and complex Fourier series to the heat conduction and Navier's equations. Jabbari et al. [11] studied the nonaxisymmetric mechanical and thermal stresses in Functionally Graded Porous Piezoelectric Material(FGPPM) hollow cylinder. Poultangari et al. [12] presented a solution for the functionally graded hollow spheres under nonaxisymmetric thermomechanical loads. Ootao and Tanigawa [13] presented the transient thermoelastic problem of functionally graded thick strip due to nonuniform heat supply. They obtained the exact solution for the two dimensional temperature change in a transient state and thermal stress of a simply supported strip under the of plain strain. Alibeigloo and Chen [14] obtained the elasticity solution for an FGM cylindrical panel integrated with piezoelectric layers. Dai [15] presented an analytical solution for electro- magneto- thermoelastic behaviors of a functionally graded piezoelectric hollow cylinder. Chen et al. [16] presented 3D free vibration analysis of a functionally graded piezoelectric hollow cylinder filled with compressible fluid. He et al. [17] derived the active control of FGM plates with integrated piezoelectric sensors and actuators. Wu et al. [18] obtained an exact solution for functionally graded piezothermoelastic cylindrical shell as sensors or actuators. Fesharaki et al. [19] presented 2D solution for electro-mechanical behavior of functionally graded piezoelectric hollow cylinder. By using the separation of variables method and complex Fourier series, the Navier equations in term of displacements are derived and solved. Eslami et al. [20] obtained an exact solution for thermal and mechanical stresses in a functionally graded thick sphere. Dai and Fu [21] developed the magneto thermo elastic interactions  in hollow structures  of functionally graded material subjected to mechanical loads. Yas and Sobhani Aragh [22] studied the three-dimensional analysis for thermo elastic response of functionally graded fiber reinforced cylindrical panel. Peng and Li [23] showed the thermal stress in rotating functionally graded hollow circular disks .Asghari and Ghafoori [24] investigated the three-dimensional elasticity solution for functionally graded rotating disks. Khoshgoftar et al. [25] presented the thermoelastic analysis of a thick walled cylinder made of functionally graded piezoelectric material. By using the separation of variables. Dube et al. [26] depicted the exact solution for electro thermo mechanical radially polarized circular cylindrical shell panel in cylindrical bending under electrostatic excitation and thermal fields. Dumir et al. [27] presented an analytical solution for piezoelectric orthotropic cylindrical panel in cylindrical bending with simply supported boundary conditions.They used the Fourier series to satisfying the simply supported boundary conditions along longitudinal edges. Akbari et al. [28] carried out three-dimensional thermo-elastic analysis of a functionally graded cylindrical shell with piezoelectric layers by differential quadrature method. Heyliger [29] carried out an exact three-dimensional analysis of a laminated piezoelectric cylinder under static loads with simply supported boundary conditions and found the elastic and electric fields of each layer of the laminate, using the Frobenious method. Chen and Shen [30] obtained the exact solution of an orthotropic cylindrical shell of finite length with piezoelectric layers acting as sensor and actuator subjected to axisymmetric thermo-electro-mechanical loads. In their study, the axisymmetric thermal and mechanical loadings were expanded as Fourier series and the power series expansion method were employed to obtain the solution. Shakeri et al. [31] carried out three-dimensional elasticity analysis of laminated cylinders with piezoelectric sensors and actuator layers, subjected to internal pressure loading and uniform electric excitation at the outer surface employing the Galerkin element method. A numerical analysis of piezoelectric strip under the effect of symmetric pressure and voltage on the upper and the lower edges with traction-free boundaries using the generalized differential quadrature method is presented by Hong et al. [32]. Shao et al. [33] carried out an analytical stress analysis of a functionally graded hollow cylinder of finite length and simply supported boundary conditions subjected to pressure loadings on the inner and outer surface. They assumed that thermo-mechanical properties of functionally graded material to be temperature dependent and vary continuously in the radial direction and employed Laplace transform techniques and series solving method to solve the ordinary differential equation. Ootao and Tanigawa [34] calculated transient thermal stresses in a cylindrical panel made of functionally graded material due to a nonuniform heat supply by analytical method. Tutuncu [35] obtained stress and displacement fields in thick walled cylinders made of functionally graded materials with exponentially varying properties subjected to internal pressure, using the power series solution method. Shao an Ma [36] calculated thermo-mechanical stresses in functionally graded circular hollow cylinders subjected to mechanical loads and linearly increasing boundary temperature, employing the Laplace transform technique and series solving method. Obata and Noda [37] carried out one-dimensional thermal stress analysis of a hollow circular cylinder  and a hollow sphere made of functionally graded materials under a steady state condition using the perturbation method. Shao [38] presented solutions for

temperature, displacement and stress fields in a functionally graded hollow cylinder using a multi-layered approach based on the theory of laminated composites. Alibeigloo [39] obtained thermo-elastic solution for axisymmetric deformation of functionally graded cylindrical shell bonded to thin piezoelectric layers assuming a Navier type solution for the governing equations. Jabbari et al [40] investigated on one-dimensional moving heat source in a hollow FGM cylinder. A direct method of solution of Navier equation is presented.

In this paper, an analytical method is presented for thermal stresses and electrical and mechanical displacements analysis for a three layers hollow cylinder made of Piezoelectric-FGM-Piezoelectric under a one-dimensional steady-state temperature distribution. The material properties, except the Poisson's ration are assumed to be varied along radial direction by power function in r. The temperature distribution is assumed to be a function of radius with general thermal and mechanical boundary conditions on the inside and outside surfaces. The input voltage to the actuator is supplied with the output voltage of the sensor. By using the separation of variables method and complex Fourier series, the Navier equations in term of displacements are derived and solved. The effect of the graded index(m) and shear modulus on the thermal stresses and electrical and mechanical displacements are investigated.

## 2    MATERIAL AND METHODS
### 2.1 Governing Equation

Consider a hollow cylinder with three layers made of Piezoelectric-FGM-Piezoelectric as shown in Fig.1. Asymmetric cylindrical coordinates $(r,\theta)$ are considered along the radial direction. The cylinder's material is graded through the *r*-direction thus the material properties are function of *r*.
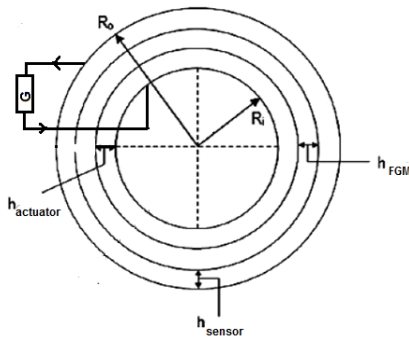


**Fig.1**
Geometry and coordinates of the laminated plate

The heat conduction equation in steady-state condition for one-dimensional problem in polar coordinates for hollow cylinder is

$$\frac{1}{r}\frac{d}{dr}\left[r\,k\,(r)\frac{dT\,(r)}{dr}\right]=0 \tag{1}$$

where $T(r)$ is temperature distribution and $k(r)$ is the thermal conduction coefficient.

The nonhomogeneous thermal conduction coefficient $k(r)$ that is a power function of *r* for piezo and FGM layers are assumed as:

$$k(r)=\begin{cases} k_{rp}(r)=k_p\,, & r_1<r<r_2\ \&\ r_3<r<r_4 \\ k_{rf}(r)=k_0r^m\,, & r_2<r<r_3 \end{cases} \tag{2}$$

where $k_0$ and m are material parameters, $k_{rp}$ and $k_{rf}$ are thermal conductivity constants for piezo and FGM, respectively. By using Eqs.(2), the heat conduction Eq. (1) for FGM and piezo layer respectively becomes

$$\frac{1}{r}\frac{d}{dr}\left[r^{m+1}k_0\frac{dT\left(r\right)}{dr}\right]=0 \tag{3a}$$

$$\frac{k_p}{r}\frac{d}{dr}\left[r\frac{dT\left(r\right)}{dr}\right]=0 \tag{3b}$$

Integrating (3a) and (3b) twice for FGM and piezo layers, separately yields

$$T\left(r\right)=\begin{cases}T^{a,s}\left(r\right)=C_1^{a,s}r^{-1}+C_2^{a,s}\,,r_1<r<r_2\ \&\ r_3<r<r_4\\T^{F}\left(r\right)=C_1^{F}r^{-(m+1)}+C_2^{F}\,,r_2<r<r_3\end{cases} \tag{4}$$

where $T^{F}$ and $T^{a,s}$ are temperature of FGM and piezo layers. Here, the suffixes "a" and "s" are used to denote the actuator and sensor layer, respectively. All the unknowns can be evaluated through satisfying thermal boundary conditions as:

$$T^{a}\left(r_1\right)=T_1\qquad,\qquad T^{s}\left(r_4\right)=T_2 \tag{5}$$

and the continuity conditions on the interfaces as:

$$T^{a}\left(r_2\right)=T^{F}\left(r_2\right)\rightarrow k_p\frac{dT^{a}}{dr}=k_m r^{m}\frac{dT^{F}}{dr} \tag{6}$$

$$T^{F}\left(r_3\right)=T^{s}\left(r_3\right)\rightarrow k_m r^{m}\frac{dT^{F}}{dr}=k_p\frac{dT^{s}}{dr} \tag{7}$$

*2.2 Stress analysis*
*2.2.1 Piezoelectric layers*

Consider $u^{a,s}$ and $\varphi^{a,s}$ be displacement components in the radial ($r$) and the electric potential, respectively (the suffixes "a" and "s" denotes actuator and sensor). Then, the strain-displacement relations and electric field-electric potential relations are

$$\varepsilon_{rr}^{a,s}=\frac{\partial u^{a,s}}{\partial r}\qquad,\qquad \varepsilon_{\theta\theta}^{a,s}=\frac{u^{a,s}}{r}\qquad,\qquad E_r^{a,s}=-\frac{\partial\varphi^{a,s}}{\partial r} \tag{8}$$

The stress-strain relations for the FGM and piezoelectric cylinder for asymmetric condition are

$$\sigma_{rr}^{a,s}=c_{11}\varepsilon_{rr}^{a,s}+c_{12}\varepsilon_{\theta\theta}^{a,s}-e_{11}E_r^{a,s}-\alpha T^{a,s}\left(r\right) \tag{9a}$$

$$\sigma_{\theta\theta}^{a,s}=c_{12}\varepsilon_{rr}^{a,s}+c_{22}\varepsilon_{\theta\theta}^{a,s}-e_{21}E_r^{a,s}-\alpha T^{(a,s)}\left(r\right) \tag{9b}$$

$$D_{rr}^{a,s}=e_{11}\varepsilon_{rr}^{a,s}+e_{21}\varepsilon_{\theta\theta}^{a,s}+\eta_{11}E_r^{a,s}+P_r T^{(a,s)}\left(r\right) \tag{9c}$$

where $\sigma_{ij}$ and $\varepsilon_{ij}\left(i,j=r,\theta\right),c_{ij}$ and $e_{ij}\left(i,j=1,2\right),\eta_{ij}\left(i,j=1,2\right),D_i$ and $P_i\left(i=r\right),\alpha$ are stress strain tensors, elastic and piezoelectric coefficients , dielectric constants, radial electric displacement, pyroelectric constant and thermal modulus, respectively. Here, the suffixes "a" and "s" are used to denote the actuator and sensors layer, respectively.

The equilibrium equations in the radius direction, irrespective of the body force and the inertia terms is expressed as:

$$\frac{\partial \sigma_{rr}^{a,s}}{\partial r} + \frac{\sigma_{rr}^{a,s} - \sigma_{r\theta}^{a,s}}{r} = 0 \tag{10}$$

In absence of free charge density, the charge equation of electrostatic is

$$\frac{\partial D_{rr}^{a,s}}{\partial r} + \frac{D_{rr}^{a,s}}{r} = 0 \tag{11}$$

Solving Eq. (11), yields

$$D_{rr}^{a,s}(r) = \frac{B_1^{a,s}}{r} \tag{12}$$

where $B_1^{a,s}$ is an unknown constant. Using Eq. (12), Eq. (9c) may be rewritten as:

$$\frac{\partial \varphi^{a,s}}{\partial r} = \frac{e_{11}}{\eta_{11}} \frac{\partial u^{a,s}}{\partial r} + \frac{e_{21}}{\eta_{11}} \frac{u^{a,s}}{r} - \frac{1}{\eta_{11}} \frac{B_1^{a,s}}{r} + \frac{P}{\eta_{11}} T^{a,s}(r) \tag{13}$$

Substituting Eq. (13) into Eqs. (9a), (9b), yields

$$\sigma_{rr}^{a,s} = (c_{11} + \frac{e_{11}e_{11}}{\eta_{11}}) \frac{\partial u^{a,s}}{\partial r} + \left( c_{12} + \frac{e_{21}e_{11}}{\eta_{11}} \right) \frac{u^{a,s}}{r} - \frac{e_{11}}{\eta_{11}} \frac{B_1^{a,s}}{r} + \left( \frac{Pe_{11}}{\eta_{11}} - \alpha \right) T^{a,s}(r) \tag{14a}$$

$$\sigma_{\theta\theta}^{a,s} = \left( c_{12} + \frac{e_{11}e_{21}}{\eta_{11}} \right) \frac{\partial u^{a,s}}{\partial r} + (c_{22} + \frac{e_{21}e_{21}}{\eta_{11}}) \frac{u^{a,s}}{r} - \frac{e_{21}}{\eta_{11}} \frac{B_1^{a,s}}{r} + \left( \frac{Pe_{21}}{\eta_{11}} - \alpha \right) T^{a,s}(r) \tag{14b}$$

Substituting Eqs. (14a),(14b) into Eq. (10), the basic displacement equation of a transversely isotropic piezoelectric hollow cylinder is expressed as:

$$H_1 \frac{\partial^2 u^{a,s}}{\partial r^2} + \frac{H_2}{r} \frac{\partial u^{a,s}}{\partial r} + \frac{H_3}{r^2} u^{a,s} + H_4 \frac{\partial T^{a,s}}{\partial r} + \frac{H_5}{r} T^{a,s} + \frac{B_1^{a,s}}{r^2} H_6 = 0 \tag{15}$$

where

$$H_1 = (c_{11} + \frac{e_{11}e_{11}}{\eta_{11}}) \qquad , \qquad H_2 = \left( (c_{11} - c_{12}) + \frac{e_{11}e_{11} - e_{11}e_{21}}{\eta_{11}} \right)$$

$$H_3 = \left( (c_{12} - c_{22}) + \frac{e_{21}e_{11} - e_{21}e_{21}}{\eta_{11}} \right) \quad , \quad H_4 = \left( \frac{P}{\eta_{11}} \right) \tag{16}$$

$$H_5 = \frac{P(e_{11} - e_{21})}{\eta_{11}} \qquad , \qquad H_6 = \frac{e_{21} - e_{11}}{\eta_{11}}$$

### 2.2.2 FGM Layers

The host structure's material is graded through the *r*-direction, thus the material properties are functions of *r*.

Let $u^F$ be the displacement component in the radial direction(the suffixes "F" is used to denote the FGM layer. Then the strain–displacement relations are

$$\varepsilon_{rr}^F = \frac{\partial u^F}{\partial r} \qquad , \qquad \varepsilon_{\theta\theta}^F = \frac{u^F}{r} \tag{17}$$

The stress-strain relations one-dimensional in the FGM plane-strain hollow cylinder are

$$\sigma_{rr}^F = (\lambda + 2\mu)\varepsilon_{rr}^F + \lambda\varepsilon_{\theta\theta}^F - (3\lambda + 2\mu)\alpha T^F(r)$$
$$\sigma_{\theta\theta}^F = (\lambda + 2\mu)\varepsilon_{\theta\theta}^F + \lambda\varepsilon_{rr}^F - (3\lambda + 2\mu)\alpha T^F(r) \tag{18}$$

where $\sigma_{ii}$ and $\varepsilon_{ii}$ $(i, j = r, \theta)$ are the stress and strain tensors, $T(r)$ is the temperature distribution determined from the heat conduction equation, $\alpha$ is the coefficient of thermal expansion, and $\lambda$ and $\mu$ are the Lame coefficients related to modulus of elasticity $E$ and Poisson's ratio $\nu$ as:

$$\lambda = \frac{\nu E}{(1+\nu)(1-2\nu)} \qquad , \qquad \mu = \frac{E}{2(1+\nu)} \tag{19}$$

The equilibrium equation in the radial direction, disregarding the body force and the inertia term, is

$$\frac{\partial \sigma_{rr}^F}{\partial r} + \frac{\sigma_{rr}^F - \sigma_{\theta\theta}^F}{r} = 0 \tag{20}$$

To obtain the equilibrium equations in terms of the displacement components for the FGM layer, the functional relationship of the material properties must be known. Because the cylinder materials is assumed to be graded along the $r$-direction, the modulus of elasticity and coefficient of thermal expansion are assumed to be described with the power laws as:

$$\alpha(r) = \alpha_0 r^m \qquad , \qquad E(r) = E_0 r^m \tag{21}$$

where $E_0$ and $\alpha_0$ are the material constants and $m$ is the power law indices of the material. We may further assume that Poisson's ratio is constant.

Using relations (17)–(21), the Navier equation in term ofthe displacement is

$$\frac{\partial^2 u^F}{\partial r^2} + \frac{(m+1)}{r}\frac{\partial u^F}{\partial r} + \frac{1}{r^2}\left(\frac{\nu m}{1-\nu} - 1\right)u^F = \alpha_0\left(\frac{1+\nu}{1-\nu}\right)r^{m-1}\left[2mT^F(r) + r\frac{\partial T^F(r)}{\partial r}\right] \tag{22}$$

## 3 ANALYTICAL SOLUTION
### 3.1 Piezoelectric layers

By substituting Eq. (4) into Eq. (15) then, the following differential equation for electrothermoelastic analysis is obtained.

$$\frac{\partial^2 u^{a,s}}{\partial r^2} + \frac{H_2}{H_1 r}\frac{\partial u^{a,s}}{\partial r} + \frac{H_3}{H_1}\frac{u^{a,s}}{r^2} = \left(\frac{H_4 C_1^{a,s} - H_5 C_1^{a,s}}{H_1}\right)r^{-1} - \frac{H_5 C_2^{a,s}}{H_1} - \frac{H_6}{H_1}B_1^{a,s} r^{-2} \tag{23}$$

Firstly, assuming that the homogeneous solution of Eq. (23) is

$$u_g^{a,s}(r) = B^{a,s} r^{\eta} \tag{24}$$

Substituting Eq. (24) into Eq. (23), the characteristic equation is obtained as follows

$$\eta^2 + \frac{H_2}{H_1}\eta + \frac{H_3}{H_1} = 0 \tag{25}$$

Eq. (25) has two real roots $\eta_1$ and $\eta_2$ :

$$\eta_{1,2} = \frac{-\dfrac{H_2}{H_1} \pm \sqrt{(\dfrac{H_2}{H_1})^2 - \dfrac{4H_3}{H_1}}}{2} \tag{26}$$

So the homogeneous solution of Eq. (23) is

$$u_g^{a,s}(r) = B_2^{a,s} r^{\eta_1} + B_3^{a,s} r^{\eta_2} \tag{27}$$

The particular solution of Eq. (23) is assumed to have the form

$$u_p^{a,s}(r) = D_1^{a,s} + D_2^{a,s} r + D_3^{a,s} r^2 \tag{28}$$

After substitution of the assumed particular solution and its derivatives into Eq. (23), $D_i^{a,s}$ ($i = 1,2,3$) are found:

$$D_1^{a,s} = -\frac{H_6}{H_3} B_1^{a,s} \tag{29}$$

$$D_2^{a,s} = \frac{(H_4 - H_5)C_1^{a,s}}{H_2 + H_3} \tag{30}$$

$$D_3^{a,s} = -\frac{H_5 C_2}{2H_1 + 2H_2 + H_3} \tag{31}$$

The complete solution for $u^{a,s}(r)$ is the sum of the general and particular solutions as:

$$u^{a,s}(r) = u_g^{a,s}(r) + u_p^{a,s}(r) \tag{32}$$

Thus,

$$u^{a,s}(r) = B_2^{a,s} r^{\eta_1} + B_3^{a,s} r^{\eta_2} + D_1^{a,s} + D_2^{a,s} r + D_3^{a,s} r^2 \tag{33}$$

Then using Eqs. (13), (14a), and (14b) yields:

$$\sigma_{rr}^{a,s}(r) = B_2^{a,s} A_1 r^{\eta_1 - 1} + B_3^{a,s} A_1 r^{\eta_2 - 1} + A_2 r^{-1} + \left(3D_3^{a,s}\right) A_1 r + \left(2D_2^{a,s} A_1 + C_2^{a,s} \frac{Pe_{11} - \alpha \eta_{11}}{\eta_{11}}\right) \tag{34}$$

$$\sigma_{\theta\theta}^{a,s}(r) = B_2^{a,s} A_3 r^{\eta_1-1} + B_3^{a,s} A_3 r^{\eta_2-1} + A_4 r^{-1} + \left(3D_3^{a,s}\right)A_3 r + \left(2D_2^{a,s} A_3 + C_2^{a,s}\,\frac{Pe_{21}-\alpha\eta_{11}}{\eta_{11}}\right) \tag{35}$$

$$\varphi^{a,s}(r) = B_2^{a,s} A_5 r^{\eta_1} + B_3^{a,s} A_6 r^{\eta_2} + A_7^{a,s} r + A_8^{a,s}\,lnr + A_9^{a,s} r^2 \tag{36}$$

where

$$A_1 = \left(\frac{e_{11}e_{11}+e_{11}e_{12}}{\eta_{11}}+(c_{11}+c_{12})\right) \qquad , \qquad A_2 = \left(\frac{D_1\left(c_{12}\eta_{11}+e_{21}e_{11}\right)-B_1^{a,s}e_{11}+(Pe_{11}-\alpha\eta_{11})C_1^{a,s}}{\eta_{11}}\right)$$

$$A_3 = \left(\frac{e_{11}e_{21}+e_{21}e_{12}}{\eta_{11}}+(c_{21}+c_{22})\right) \qquad , \qquad A_4 = \left(\frac{D_1\left(c_{22}\eta_{11}+e_{21}e_{21}\right)-B_1^{a,s}e_{21}+(Pe_{21}-\alpha\eta_{11})C_1^{a,s}}{\eta_{11}}\right) \tag{37}$$

$$A_5 = \frac{e_{11}+e_{21}\eta_1^{-1}}{\eta_{11}} \qquad , \qquad A_6 = \frac{e_{11}+e_{21}\eta_2^{-1}}{\eta_{11}} \qquad , \qquad A_7 = D_2^{a,s}\left(\frac{e_{11}+e_{21}}{\eta_{11}}\right)+C_2^{a,s}\,\frac{P}{\eta_{11}}$$

$$A_8 = D_1^{a,s}\,\frac{e_{21}}{\eta_{11}}-\frac{B_1^{a,s}}{\eta_{11}}+\frac{PC_1^{a,s}}{\eta_{11}} \qquad , \qquad A_9 = \frac{D_3^{a,s}\left(2e_{11}+e_{21}\right)}{2\eta_{11}}$$

*3.2 FGM layer*

Substituting Eq. (4) into Eq. (22) yields

$$\frac{\partial^2 u^F}{\partial r^2}+\frac{(m+1)}{r}\frac{\partial u^F}{\partial r}+\frac{1}{r^2}\left(\frac{vm}{1-v}-1\right)u^F = \alpha_0\left(\frac{1+v}{1-v}\right)\left[(m-1)C_1^F r^{-2}+2mC_2^F r^{m-1}\right] \tag{38}$$

Eq. (38) is the Euler differential equation with general and particular solutions. The general solution is assumed to have the form

$$u_g^F(r) = B^F r^\gamma \tag{39}$$

Substituting Eq. (39) into Eq. (38) yields

$$\gamma^2+(m+1)\gamma+\left(\frac{vm}{1-v}-1\right)=0 \tag{40}$$

Eq. (40) has two real roots $\gamma_1$ and $\gamma_2$ :

$$\gamma_{1,2} = \frac{-(m+1)\pm\sqrt{(m+1)^2-4\left(\frac{vm}{1-v}-1\right)}}{2} \tag{41}$$

Thus, the general solution is

$$u_g^F(r) = B_1^F r^{\gamma_1}+B_2^F r^{\gamma_2} \tag{42}$$

The particular solution $u_p^F(r)$ is assumed to be of the form

$$u_p^F(r) = D_1^F + D_2^F r^{m+1} \tag{43}$$

Substituting Eq. (43) into Eq. (38), and then equating the coefficients of the identical powers yields

$$D_1^F = \frac{\alpha_0 (m-1) C_1^F [\frac{1+\nu}{1-\nu}]}{2[\frac{\nu m}{1-\nu} - 1]} \tag{44}$$

$$D_2^F = \frac{2\alpha_0 m C_2^F [\frac{1+\nu}{1-\nu}]}{[m(m+1) + (m+2)(m+1) + 2(\frac{\nu m}{1-\nu} - 1)]} \tag{45}$$

The complete solution for $u^F(r)$ is the sum of the general and particular solutions as:

$$u^F(r) = u_g^F(r) + u_p^F(r) \tag{46}$$

Thus,

$$u^F(r) = B_1^F r^{\gamma_1} + B_2^F r^{\gamma_2} + D_1^F + D_2^F r^{m+1} \tag{47}$$

Substituting Eq. (47) into Eqs. (18), the stresses are obtained as:

$$\sigma_{rr}^F = B_1^F \left[ \lambda(\gamma_1 + 2) + 2\mu\gamma_1 \right] r^{\gamma_1 - 1} + B_2^F \left[ \lambda(\gamma_2 + 2) + 2\mu\gamma_2 \right] r^{\gamma_2 - 1} + D_1^F \left[ 2\lambda - (3\lambda + 2\mu)\alpha_0 C_1^F \right] r^{-1}$$
$$+ D_2^F \left[ \lambda(m+3) + 2\mu(m+1) - (3\lambda + 2\mu)\alpha_0 C_2^F \right] r^m \tag{48}$$

$$\sigma_{\theta\theta}^F = B_1^F \left[ \lambda(\gamma_1 + 2) + 2\mu \right] r^{\gamma_1 - 1} + B_2^F \left[ \lambda(\gamma_2 + 2) + 2\mu \right] r^{\gamma_2 - 1} + D_1^F \left[ 2(\lambda + \mu) - (3\lambda + 2\mu)\alpha_0 C_1^F \right] r^{-1}$$
$$+ D_2^F [\lambda(m+3) + 2\mu - (3\lambda + 2\mu)\alpha_0 C_2^F] r^m \tag{49}$$

*3.3 Boundary& continuity conditions*

It is obvious that once the unknown parameters $B_1^F, B_2^F, B_1^{a,s}, B_2^{a,s}, B_3^{a,s}$ and $B_4^{a,s}$ can be evaluated through satisfying the boundary conditions and continuity requirements on the interface. Therefore, displacements, electric potential, stress and other responses can be evaluated. The corresponding boundary conditions can be written as:

$$\sigma_{rr}^a(r = r_1) = -p_1 \quad , \quad \sigma_{rr}^s(r = r_4) = -p_2 \tag{50}$$

For sensor layer

$$\varphi^s(r = r_3) = 0 \quad , \quad D_{rr}^s(r = r_4) = 0 \tag{51}$$

For actuator layer

$$\varphi^a(r = r_1) = V^a \quad , \quad \varphi^a(r = r_2) = 0 \tag{52}$$

where $p_1$ and $p_2$ are the inner and outer pressure, respectively. $V^s$ is the output voltage of the sensor layer as:

$$V^s = \varphi^s \qquad (r = r_4) \tag{53}$$

Then ,the output voltage of the sensor $V^s$ is feeded into the control algorithm, and $V^a$ (the input voltage to the actuator layer) is obtained as follows:

$$V^a = GV^s \tag{54}$$

Here, *G* is the feedback gain. In addition, those of continuity requirements for the stresses and displacements on the interfaces must be satisfied .Therefore, we have

$$\sigma_{rr}^a (r = r_2) = \sigma_{rr}^F (r = r_2) \quad , \qquad \sigma_{rr}^F (r = r_3) = \sigma_{rr}^s (r = r_3) \tag{55}$$

$$u^a (r = r_2) = u^F (r = r_2) \quad , \qquad u^F (r = r_3) = u^s (r = r_3) \tag{56}$$

## 4   RESULTS AND DISCUSSION

Assume material properties for piezoelectric on first layer as an actuator Ba2NaNb5015  and for third layer piezoelectric as a sensor PZT-4 from the following table.

**Table1**
Material properties of piezoelectric.

| Material | Elastic constants, Gpa | | | | | | |
|---|---|---|---|---|---|---|---|
| | $c_{11}$ | $c_{12}$ | $c_{13}$ | $c_{22}$ | $c_{23}$ | $c_{33}$ | $c_{44}$ |
| PZT-4 | 139 | 78 | 74 | 139 | 74 | 115 | 25.6 |
| Ba2NaNb5015 | 239 | 104 | 5 | 247 | 52 | 135 | 65 |

**Table2**
Piezoelectric constants, $C/m^2$ Permittivity, $10^{-9}C/Nm^2$ Pyroelectric constants Coefficient of thermal $10^{-5}c/Km^2$ expansion, $1/K$ .

| | $e_{11}$ | $e_{12}$ | $e_{22}$ | $\eta_{11}$ | $\eta_{22}$ | $P_r = P_\theta = P_0$ | $\alpha_r = \alpha_\theta = \alpha_0$ |
|---|---|---|---|---|---|---|---|
| PZT-4 | -5.2 | -5.2 | 12.7 | 6.5 | 6.5 | 5.4 | 2.62 |
| Ba2NaNb5015 | -0.4 | -0.3 | 3.4 | 1.96 | 2.01 | 5.4 | 2.458 |

Let us consider a thick FGM hollow cylinder with the following geometry properties

$$r_1 = 1 \quad , \quad r_2 = 1.2 \quad , \quad r_3 = 1.4 \quad , \quad r_4 = 1.6$$

And the material properties of FGM layer are :

$$E_0 = 200Gpa \quad , \quad \alpha_0 = 1.2 \times 10^{-6} K^{-1} \quad , \quad v = 0.3 \quad , \quad k_m = 2 Wm^{-1}K^{-1}$$

As the first example, consider a thick hollow cylinder where its mechanical, thermal and electrical boundary conditions are, respectively, taken as:

$$\sigma_{rr}^a (r = r_1) = -50Mpa \quad , \quad T^a (r_1) = 0 \quad , \quad \varphi^a (r = r_1) = 0 \quad , \quad \varphi^s (r = r_3) = 0$$

$$\sigma_{rr}^s (r = r_4) = 0 \quad , \quad T^s (r_4) = 10K \quad , \quad \varphi^a (r = r_2) = 0 \quad , \quad D_{rr}^s (r = r_4) = 0$$
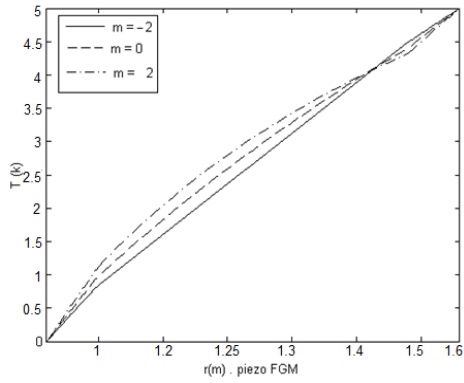
**Fig.2**
Temperature distribution in the piezo FGM hollow cylinder hollow cylinder with various *m*.
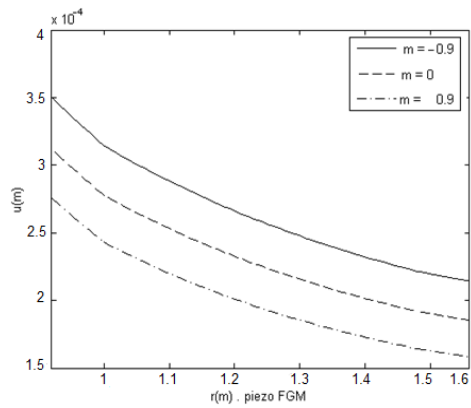


**Fig.3**
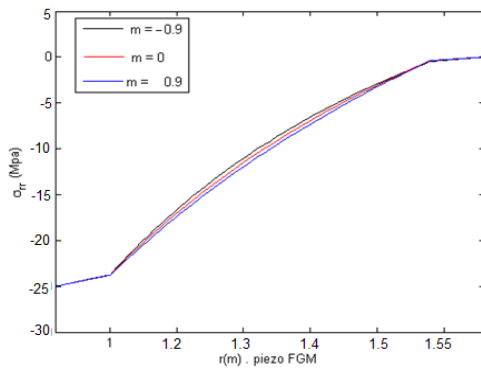Radial displacement distribution in the piezo FGM hollow cylinder with various *m*.



**Fig.4**
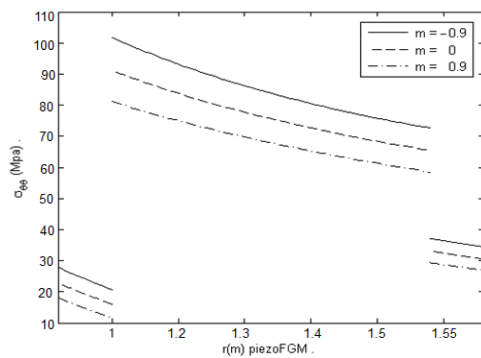Radial stress distribution in the piezo FGM hollow cylinder with various *m*.



**Fig.5**
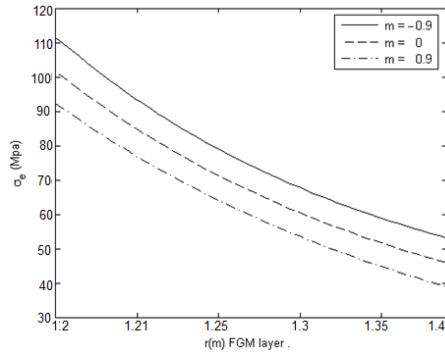Circumferential stress distribution in the piezo FGM hollow cylinder with various *m*.

**Fig.6**
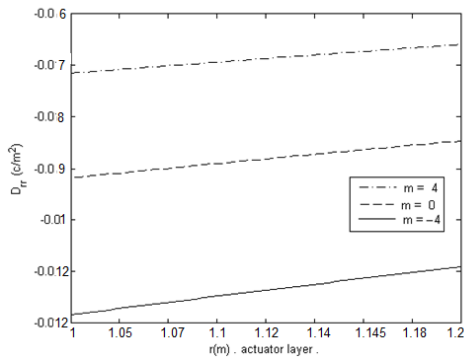Effective stress distribution in the FGM layer with various *m* .



**Fig.7**
Radial electrical displacement in the actuator layer with various *m*.
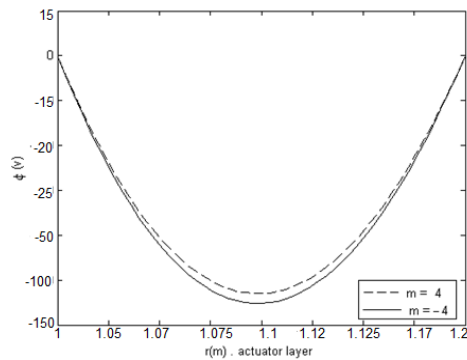


**Fig.8**
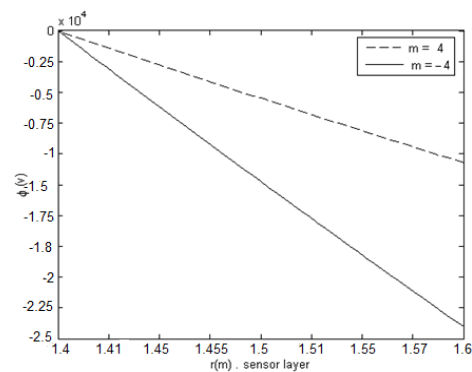Electric potential distribution in the actuator layer with various *m*.



**Fig.9**
Electric potential distribution in the sensor layer with various *m*.

For different values of *m* , temperature profile, radial displacement, radial stresses,circumferential stresses, effective stress, electric potential and radial electrical displacement along the radial direction are plotted in Figs. 2-9. From Fig. 2, it is seen easily that the temperatures at the internal and external boundaries which satisfy the prescribed thermal boundary conditions, the temperature increases as the graded index *m* increases at the more

same radial point. From Fig. 3, one knows, the radial- displacement decreases gradually from inner surface to outer surface of the smart FGM hollow cylinder, the radial displacement decreases as the graded index $m$ increases at the same radial point. It is seen easily from Fig.4 that the radial stresses at the internal and external boundaries which satisfy the given mechanical boundary conditions, the radial stress decreases as the graded index $m$ increases at the same radial point.The distribution of circumferential stress is shown in Fig. 5, similar patterns is observed from this figure too. Fig. 6 shows the effective stress distributions with various $m$, here, lower power law indices produce more effective stress along the radius.

Fig. 7 shows radial electrical displacement distributions with various $m$. It is seen easily from Fig. 7 that radial electrical displacement decreases as the graded index $m$ decreases at the same radial point.The distribution of electric potential in actuator and sensor layers are shown in Figs. 8 and 9, respectively. It is seen easily from Figs. 8 and 9 that electric potential satisfie sthe prescribed electrical boundary conditions.Similar to the radial electrical displacement ,the distribution of Electric potential decreases as the graded index $m$ decreases at the same radial point.

In this example, smart FGM structure ( Fig.1) that , the outer and inner piezoelectric layers serve, respectively, as sensor and actuator which are linked by constant gain control algorithm, and its thermal, mechanical and electrical boundary conditions are, respectively, taken as:

$$T^a\left(r_1\right)=0K \quad , \quad T^s\left(r_4\right)=20k \quad , \quad \varphi^s\left(r=r_3\right)=0 \quad , \quad \varphi^a\left(r=r_1\right)=V^a$$

$$u^a\left(r=r_1\right)=0 \quad , \quad \sigma_{rr}^s\left(r=r_4\right)=0 \quad , \quad D_{rr}^s\left(r=r_4\right)=0 \quad , \quad \varphi^a\left(r=r_2\right)=0$$

As its mentioned before, $V^a$ is the actuating voltage as determined by the control algorithm. Fig.10 shows distributions of the temperatures along the radial direction in the piezo-FGM hollow cylinder with m=1, it is seen easily that the temperatures at the internal and external boundaries which satisfy the prescribed thermal boundary conditions. Fig. 11 shows electric potential distributions with along the radial direction in sensor layer with m=1, it is seen easily from Fig. 11 that $V^s=6000V$.
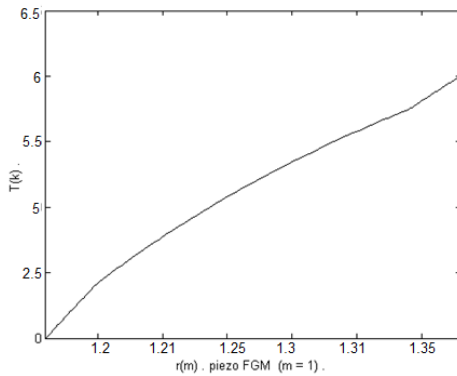


**Fig.10**
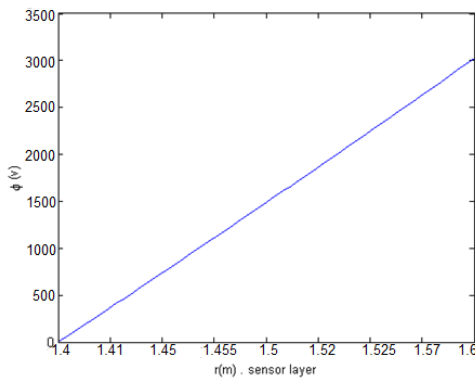Temperature distribution in the piezo FGM hollow cylinder where m=1.



**Fig.11**
Electric potential distribution in the sensor layer, where G=0 and m=1.

For different values of *G* (feedback gain),radial displacement, radial stresses,circumferential stresses,effective stress, electric potential and radial electrical displacement along the radial direction are plotted in Figs. 12-16. Here, the graded index is *m*=1. From Fig. 12, one knows, the radial displacement decreases with negative feedback gain and increases by applying the positive one . It is seen easily from Fig.13 that the radial stresses increases by applying the negative feedback gain and with the positive feedback gain, the radial stresses of the smart FGM hollow cylinder decreases.
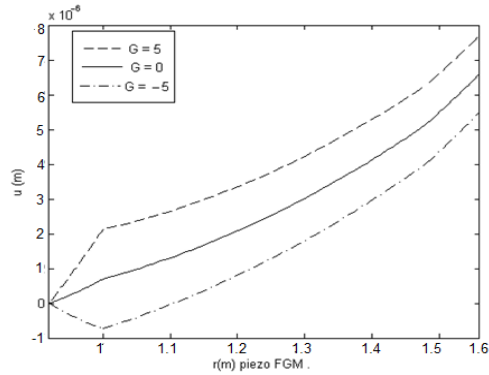


**Fig.12**
Radial displacement distribution in the piezo-FGM hollow cylinder with various *G*, where *m*=1 .
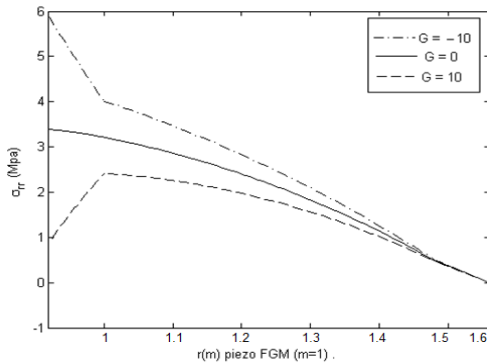


**Fig.13**
Radial stress distribution in the piezo- FGM hollow cylinder with various *G*, where *m*=1.

The distribution of circumferential stress is shown in Figs. 14(a) and 14(b) . Similar to the distribution of the radial- displacement, the circumferential stress decreases with negative feedback gain and increases by applying the positive one . Fig. 15 shows radial electrical displacement distributions with various *G* in actuator layer , it is seen easily from Fig. 15 that radial electrical displacement decreases as the feedback gain decreases at the same radial point. Fig. 16 shows electric potential distributions with various *G* in actuator layer, it is seen easily from Fig. 16 that electric potential satisfies the prescribed boundary condition.
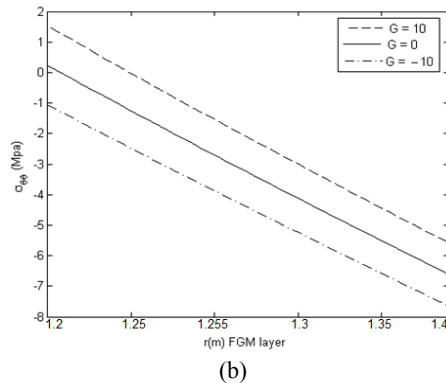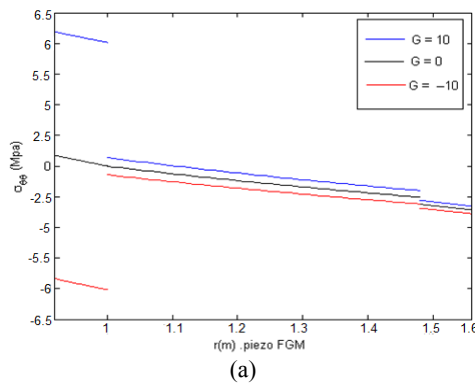


(a)



(b)

**Fig.14**
a) Circumferential stress distribution in the piezo FGM hollow cylinder various *G*, where *m*=1. b) Circumferential stress distribution in the FGM layer with various *G*, where *m*=1.
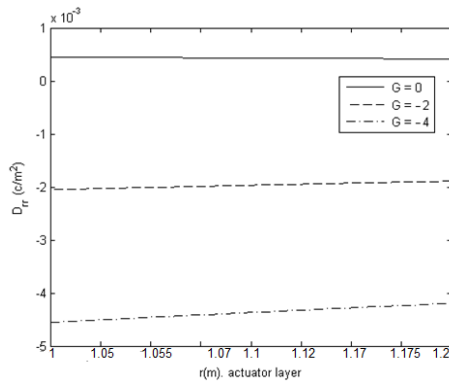
**Fig.15**
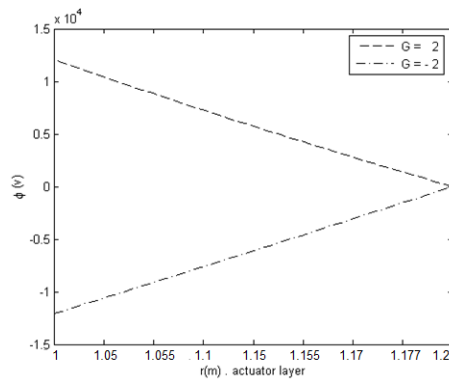Radial electrical displacement in the actuator layer with various $G$, where $m$=1 .

**Fig.16**
Electric potential distribution in the actuator layer with various $G$, where $m$=1.

## 5   CONCLUSION

In this paper, an attempt is made to study the problem of general solution for the thermal and mechanical stresses in a thick three layers piezoelectric-functionally graded materials piezoelectric hollow cylinder where the one-dimensional asymmetric steady-state loads are implied. The material properties are assumed to vary with a power-law function along the thickness of cylinder. The method of solution is based on the direct method and uses the power series, rather than the potential method and by using the complex Fourier series, the Navier equations were solved. The advantages of this method is its generality and from mathematical point of view, any type of the mechanical and thermal boundary conditions can be considered without any restrictions. Beware that this method does not have the mathematical problems to solve the general types of boundary conditions which are usually happened in the potential function method. By using this method and considering the special boundary conditions and material properties for piezoelectric-FGM-piezoelectric hollow cylinder, the mechanical and electrical displacements and stresses can be controlled and optimized to design and use this kind of structures.
It is concluded that:

Numerical results in example.1.show that the graded index $m$ has a great effect on the piezo-thermoelectric behavior of a Smart FGM hollow cylinder, and adopting a certain value of the $m$ can optimize the responses. The stress decreases as the graded index $m$ increases. It is possible for engineers to design Smart FGM cylindrical structures that can meet some special requirements.

It can be concluded that it is possible to active control of stresses displacement by applying a suitable feedback gain .This will be of particular importance in modern engineering design.

By increasing the positive feedback gain on piezo-FGM hollow cylinder, radial displacement increases and by negative feedback gain radial displacement reduces. But the effect of feedback gain on radial stresses is inverse.

## REFERENCES

[1]     Wu C. P., Syu Y. S., 2007, Exact solutions of functionally graded piezoelectric shells under cylindrical bending, *International Journal of Solids and Structures* **44**: 6450-6472.

[2]     Wang H.M., Xu Z.X. , 2010, Effect of material inhomogeneity on electromechanical behaviors of functionally graded piezoelectric spherical structures, *Computational Materials Science* **48**: 440-445.

[3]     Li X.Y., Ding H.J., Chen  W.Q., 2008, Elasticity solutions for a transversely isotropic functionally graded circular plate subject to an axisymmetric transverse load qrk, *International Journal of Solids* and *Structures* **45**:191-210.

[4]     Tiersten HF., 1969,  *Linear Piezoelectric Plate Vibrations*, New York, Plenum Press.

[5]     Kapuria S., Dumir PC., Sengupta S., 1996,  Exact piezothermoelastic axisymmetric solution of a finite transversely isotropic cylindrical shell, *Computers & Structures* **61**:1085-1099.

[6]     Lutz M.P., Zimmerman R.W., 1996, Thermal stresses and effective thermal expansion coefficient of functionally graded sphere, *Journal of Thermal Stresses* **19**: 39-54.

[7]     Zimmerman R.W., Lutz M.P., 1999, Thermal stresses and thermal expansion in a uniformly heated functionally graded cylinder, *Journal of Thermal Stresses* **22**:177-188.

[8]     Jabbari M., Sohrabpour S., Eslami M.R., 2003, General solution for mechanical and thermal stresses in functionally graded hollow cylinder due to radially symmetric loads, *Journal of Applied Mechanics* **70**:111-118.

[9]     Jabbari M., Sohrabpour S., Eslami M.R., 2002, Mechanical and thermal stresses in a functionally graded hollow cylinder due to radially symmetric loads, *International Journal Pressure Vessels and Piping* **79**: 493-497.

[10]    Jabbari M., Bahtui A., Ealami M.R., 2009, Axisymmetric mechanical and thermal stresses in thick short length functionally graded material cylinder, *International Journal Pressure Vessels and Piping* **86**: 296-306.

[11]    Jabbari M., Meshkini M., Ealami M.R., 2012, Nonaxisymmetric mechanical and thermal stresses in functionally graded porous piezoelectric material hollow cylinder, *International Journal Pressure Vessels Technology* **134**:061212-061237.

[12]    Poultangari R., Jabbari M., Eslami M.R., 2008, Functionally graded hollow spheres under non-axisymmetric thermo-mechanical loads, *International Journal Pressure Vessels and Piping* **85**: 295-305.

[13]    Ootao Y., Tanigawa Y., 2004, Transient thermoelastic problem of functionally graded thick strip due to non uniform heat supply, *Composite Structures*  **63**(2):139-146.

[14]    Alibeigloo  A., Chen W.Q., 2010, Elasticity solution for an FGM cylindrical panel integrated with piezoelectric layers, *European Journal of Mechanics - A/Solids* **29**: 714-723.

[15]    Dai H. L., Hong L., Fu Y. M.,  Xiao X., 2010, Analytical solution for electro magnetothermoelastic behaviors of a functionally graded piezoelectric hollow cylinder, *Applied Mathematical Modeling* **34**: 343-357.

[16]    Chen W. Q., Bian Z, G., Lv C.F., Ding H.J., 2004, 3D free vibration analysis of a functionally graded piezoelectric hollow cylinder filled with compressible fluid, *International Journal of Solids and Structures* **41**: 947-964.

[17]    He X. Q., Ng T.Y., Sivashanker S., Liew k. M., 2001, Active control of FGM plates with integrated piezoelectric sensors and actuators , *International Journal of Solids and Structures* **38**:1641-1655.

[18]    Wu X. H., Shen Y. P., Chen C., 2003 , An exact solution for functionally graded piezothermoelastic cylindrical shell as sensors or actuators, *Materials Letters* **57**:3532-3542.

[19]    Fesharaki J. J., Fesharaki J. V., Yazdipoor M., Razavian B., 2012, Two-dimensional solution for electro-mechanical behavior of functionally graded piezoelectric hollow cylinder, *Applied Mathematical Modeling* **36**:5521-5533.

[20]    Eslami M.R., Babaei M.H., Poultangari R., 205, Thermal and mechanical stresses in a functionally graded thick sphere, *International Journal Pressure Vessels and Piping* **82**: 522-527.

[21]    Dai H.L., Fu Y. M. , 2007, Magnetothermoelastic interactions in hollow structures of functionally graded material subjected to mechanical loads, *International Journal Pressure Vessels and Piping*  **84**:132-138.

[22]    Yas M.H., SobhaniAragh B., 2010, Three-dimensional analysis for thermoelastic response of functionally graded fiber reinforced cylindrical panel, *Composite Structures* **92**: 2391-2399.

[23]    Peng X.L., Li X.F., 2010, Thermal stress in rotating functionally graded hollow circular disks, *Composite Structures* **92**:1896-1904.

[24]    Asghari M., Ghafoori E., 2010, A three-dimensional elasticity solution for functionally graded rotating disks, *Composite Structures*  **92**:1092-1099.

[25]    Khoshgoftar M.J., Ghorbanpour Arani A., Arefi M., 2009, Thermoelastic analysis of a thick walled cylinder made of functionally graded piezoelectric material, *Smart Materials and Structures* **18**:115007.

[26]    Dube G.P., Kapuria S., Dumir G.P., 1996, Exact piezothermoelastic solution of simply-supported orthotropic circular cylindrical panel in cylindrical bending, *Archive of Applied Mechanics* **66**: 537-554.

[27]  Dumir P.C., Dube G.P., Kapuria S., 1997, Exact piezoelectric solution of simply-supported orthotropic circular cylindrical panel in cylindrical bending, *International Journal of Solids and Structures* **34**: 685-702.

[28]  Alashti A.R., Khorsand M., 2011, Three-dimensional thermo-elastic analysis of a functionally graded cylindrical shell with piezoelectric layers by differential quadrature method , *International Journal Pressure Vessels and Piping* **88**:167-180.

[29]  Heyliger P., 1997, A note on the static behavior of simply-supported laminated piezoelectric cylinders, *International Journal of Solids and Structures* **34**:3781-3794.

[30]  Chen C.Q., Shen Y.P., 1996, Piezothermoelasticity analysis for a circular cylindrical shell under the state of axisymmetric deformation, *International Journal of Engineering Science* **34**:1585-1600.

[31]  Shakeri M., Saviz M.R., Yas M.H., 2006, Elasticity solution of laminated cylindrical shell with piezoelectric actuator and sensor layer, *Proceedings of the Eighth International Conference on Computational Structures Technology*, Spain.

[32]  Shao Z.S. , Fan L.F., Wang T.J., 2004, Analytical solutions of stresses in functionally graded circular hollow cylinder with finite length, *Key Engineering Materials* **261-263**: 651-656.

[33]  Ootao Y., Tanigawa Y., 2005, Two-dimensional thermoelastic problem of functionally graded cylindrical panel due to nonuniform heat supply, *Mechanics Research Communications* **32**:429-443.

[34]  Tutuncu N., 2007, Stresses in thick-walled FGM cylinders with exponentially-varying properties, *Engineering Structures* **29**:2032-2035.

[35]  Shao Z.S., Ma G.W., 2008, Thermo-mechanical stresses in functionally graded circular hollow cylinder with linearly increasing boundary temperature, *Composite Structures* **83**:259-265.

[36]  Obata Y., Noda N.,1994, Steady thermal stresses in a hollow circular cylinder and a hollow sphere of a functionally graded material, *Journal of Thermal Stresses* **14**:471-487.

[37]  Shao Z.S., 2005, Mechanical and thermal stresses of a functionally graded circular hollow cylinder with finite length, *International Journal Pressure Vessels and Piping* **82**:155-163.

[38]  Alibeigloo A., 2010, Thermoelastic solution for static deformations of functionally graded cylindrical shell bonded to thin piezoelectric layers, *Composite Structures* **93**:961-972.

[39]  Jabbari M., Mohazzab A.H., Bahtui A., 2009, One-dimensional moving heat sourc in a hollow FGM cylinder, *International Journal Pressure Vessels Technology* **131**:021202-021209.